J Gastrointest Surg (2013) 17:304–312
DOI 10.1007/s11605-012-2094-0

ORIGINAL ARTICLE

# Clinical Application of Image-Enhanced Minimally Invasive Robotic Surgery for Gastric Cancer: A Prospective Observational Study

**Yoo Min Kim · Song-Ee Baek · Joon Seok Lim · Woo Jin Hyung**

Received: 6 April 2012 / Accepted: 13 November 2012 / Published online: 1 December 2012


**Abstract**
*Background* This study was performed to validate the feasibility and role of image-guided robotic surgery using preoperative computed tomography (CT) images for the treatment of gastric cancer.
*Methods* Twelve patients scheduled to undergo robotic gastrectomy for gastric cancer were registered. Vessels encountered during gastrectomy were reconstructed using 3D software and their anatomical variation was evaluated using preoperatively performed CT-angiography. The vascular information was transferred to a robot console using a multi-input display mode. Radiologic findings acquired from preoperative CT by the radiologist were compared with intraoperative findings of the surgeon. This study is registered with www.clinicaltrials.gov as NCT01338948.
*Results* All 12 robotic gastrectomies were performed without any problems. All anatomical data acquired using 3D software were transferred successfully during surgery. Intraoperative vascular images depicted vasculatures around the stomach and could identify important vascular variations. During surgery, relevant vascular information led the surgeon to branch sites and facilitated lymphadenectomy around the vessels. Image-guidance during the operation provided a vascular map and enabled the surgeon to avoid accidental bleeding and damage to other organs by preventing vascular injuries.
*Conclusion* Image-guided robotic surgery for gastric cancer using preoperative CT-angiography reconstructed during operation by a surgically trained radiologist who could adjust the images by anticipating the operative procedure was feasible and improved the efficiency of surgery by eliminating the possibility of vascular injuries.

**Keywords** Image-guided surgery · Robotic gastrectomy · CT-angiography

**Electronic supplementary material** The online version of this article (doi:10.1007/s11605-012-2094-0) contains supplementary material, which is available to authorized users.

Y. M. Kim · W. J. Hyung (✉)
Department of Surgery, Yonsei University College of Medicine, 50 Yonsei-ro Seodaemun-gu, Seoul 120-752, Korea
e-mail: wjhyung@yuhs.ac

S.-E. Baek · J. S. Lim
Department of Radiology, Yonsei University College of Medicine, Seoul, Korea

W. J. Hyung
Brain Korea 21 Project for Medical Science, Yonsei University College of Medicine, Seoul, Korea

W. J. Hyung
Robot and Minimally Invasive Surgery Center, Severance Hospital, Yonsei University Health System, Seoul, Korea

## Introduction

The development of imaging tools provides the medical and surgical field with new methods for the diagnosis and treatment of disease.[1] Diagnoses through various imaging technology are replacing or supplementing invasive endoscopic and angiographic procedures.[2] By using images from computed tomography (CT) and magnetic resonance imaging (MRI), not only the disease extent, but also patient-specific anatomy can be obtained before the surgical procedure.[3] These imaging technologies are rapidly being applied to various types of complicated procedures during pretreatment planning, simulation or during intervention.[4,5]

The introduction of image-guided procedures has allowed the application of image-guided surgery in accordance with the desire for minimally invasive procedures.[3,6] Image-guided surgery is an operation in which the surgeon uses indirect visualization. Most image-guided surgical procedures are minimally invasive. Image guidance was originally developed for the treatment of brain tumors and has since found a widespread application in various types of surgery.[4,7–11] However, this technique has mostly been used for relatively fixed structures or organs that do not move during the operation according to positional changes compared with images obtained during the preoperative period. There are still technical limitations to its application for flexible tissues that can change position during the operation. In particular, the application of image-guided procedures for minimally invasive gastrectomy remains a challenge.[12–14]

In this study, we assessed the feasibility and usefulness of image-guided robotic gastrectomy with lymph node dissection. We also aimed to assess the accuracy of radiologic findings of anatomical vascular structure by comparing these findings with the surgical findings.

## Methods

### Patient and Inclusion Criteria

This prospective observational study included 12 patients scheduled to receive robotic gastrectomy for gastric cancer in Severance Hospital, Yonsei University Health System. Participants provided written informed consent for evaluation, robotic surgery, and follow-up of medical records. This study was approved by the Institutional Review Boards of Severance Hospital (4-2009-0291). This study was also registered at ClinicalTrials.gov, number NCT01338948.

The routine preoperative assessment for gastric cancer in our institute includes esophagogastroduodenoscopy (EGD), endoscopic ultrasonography (EUS), and CT. Patients who fulfilled the following criteria were enrolled: (a) older than 20 years; (b) histologically confirmed gastric adenocarcinoma; (c) wanted robotic gastric cancer surgery; (d) preoperative clinical stage I (T1N0, T1N1, T2N0) diagnosed with EGD, EUS, and CT; (e) no history of drug allergy; (f) serum creatinine level less than 1.5 times the upper normal limit.

### Outcome Measures

The possibility of an integration of reconstructed CT images to the robot console during robotic gastrectomy was assessed, and the correlation between information on vascular anatomy from CT-angiography and operative findings was evaluated. Operative outcomes including the number of retrieved lymph nodes, operation time, blood loss, surgery-related complications, and the rate of conversion to laparotomy or laparoscopy were also evaluated.

### Computed Tomographic Technique

All patients included underwent 64-detector row CT scanning (SOMATOM Sensation 64; Siemens Medical Solutions, Forchheim, Germany). Before CT scanning, all patients received 10 mg butylscopolamine bromide (Buscopan; Boehringer Ingelheim, Ingelheim, Germany) intravenously through an antecubital vein to minimize bowel peristalsis and facilitate hypotonia. One and a half packs of gas-producing crystals (total 6 g) with a minimal amount of water (<10 mL) were administered orally immediately before CT scanning to obtain gastric distention. All patients received 120–150 mL contrast material (Ultravist 300; Schering, Berlin, Germany or Omnipaque 300; GE Healthcare, Princeton, NJ, USA) intravenously using an automatic power injector at a rate of 3–4 mL/s. Scans were acquired in a craniocaudal direction with the following parameters: detector collimation of 64 rows × 0.6 mm, 0.5-s gentry rotation speed, pitch 1.0, and tube current of 120 kV (peak) and 160 mAs.

A bolus-tracking program was used to commence diagnostic CT data acquisition after the intravenous injection of a contrast agent. The region-of-interest cursor for bolus tracking was placed in the descending aorta at the level of the first lumbar vertebra for real-time serial monitoring. Early arterial and portal phase images were commenced at 6 and 55 s, respectively after the trigger (trigger threshold level, 100 HU). Axial CT images were reconstructed with a 1-mm section thickness and a 1-mm interval for 3D reconstruction, and maximum intensity projection (MIP) images were also generated from the source images.

### Image Analysis and Intraoperative Technique

#### *3D Reconstruction of CT-Angiography During Surgery*

For 3D rendering and display, 1-mm section CT datasets were transferred to a workstation. Perigastric vessels encountered during gastrectomy were reconstructed and displayed by a radiologist during the operation using 3D software (AquariusNET thin-client viewer, TeraRecon, San Mateo, CA, USA). The 3D reconstruction was performed in the operating room because deformation of a hollow viscus or soft tissue compromises image-guided surgery based on preoperative images. This was done because it is required that the preoperative images were realistically warped to match the surgical situation, such as positional changes. AquariusNET for image management enables personal computers to act as real-time post-processing diagnostic workstations. The radiologist who had observed over 20 cases of minimally invasive gastrectomy reconstructed the

images during the operation in the same direction of operative view. This was possible because the reconstruction software allows a radiologist to adjust the image in the same direction of the fixed laparoscopic view through the umbilical port as mentioned previously. The measurement of the distance from the reference points to specific vessels was made just before dissecting the target vessels because the radiologist had good understanding of gastrectomy procedure. In this study, the radiologist in the operation room adjusted the 3D reconstructed CT images of target vessels in accordance with laparoscopic orientation and operative field based on the surgical images displayed on the monitor by communicating with the surgeon during operation. The 3D volume set was manipulated using a different orientation and cut planes by adjusting the window level, center, brightness, and opacity to best demonstrate vascular structures around the stomach according to the operative view. MIP images were also used.

*Image-Guided Robotic Gastrectomy Using TilePro™*

The indications and technique of robotic radical gastrectomy were described previously.[15] A single surgeon performed routine radical gastrectomy procedures under the guidance of preoperative 3D CT images concurrent with the reconstruction of vascular images. During the operation, 3D reconstructed images from a preoperative CT scan can be integrated into the robot console and aligned with the real-time surgical view using the TilePro™ program. TilePro™ is a multi-input display mode of the Robotic surgical system (da Vinci®; Intuitive Surgical, Sunnyvale, CA, USA) that allows the surgeon to simultaneously view up to two additional images as a picture-on-picture on the robotic console screen and assistant monitors. In this way, the 3D reconstructed and/or MIP images were simultaneously presented on the surgeon console in the same direction of the real-time surgical view.

*Correlation of Vascular Anatomy*

During gastrectomy for gastric cancer, six vascular structures, left gastroepiploic vessels, right gastroepiploic artery and vein, right gastric artery, and left gastric artery and vein, were identified to dissect the lymph nodes around the vessels. The anatomic variations of these six vessels are important to prevent possible complications related to lymph node dissection during gastrectomy. Thus, the following specific points of examination for anatomic variations were investigated; omental branches of the left gastroepiploic vessels, drainage pattern of right gastroepiploic vein to gastrocolic trunk, presence and origin of infrapyloric artery, origin of right gastric artery, drainage pattern of left gastric vein, and origin of left gastric artery and its branching patterns (Figs. 1 and 2).

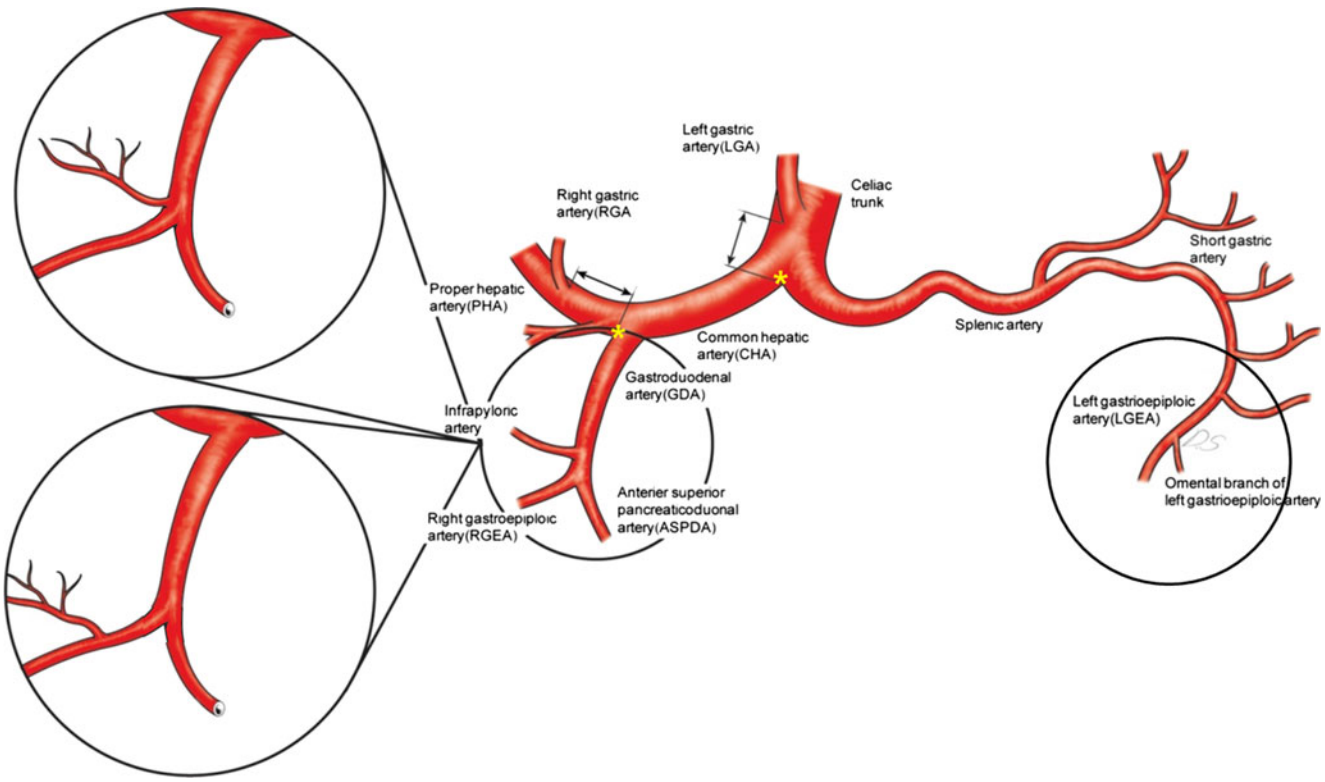


**Fig. 1** Estimation of arterial components. Arterial variations of the left gastroepiploic artery, right gastroepiploic artery, right gastric artery, and left gastric artery were evaluated, and distances from their reference points were measured (*asterisk* indicates reference point)

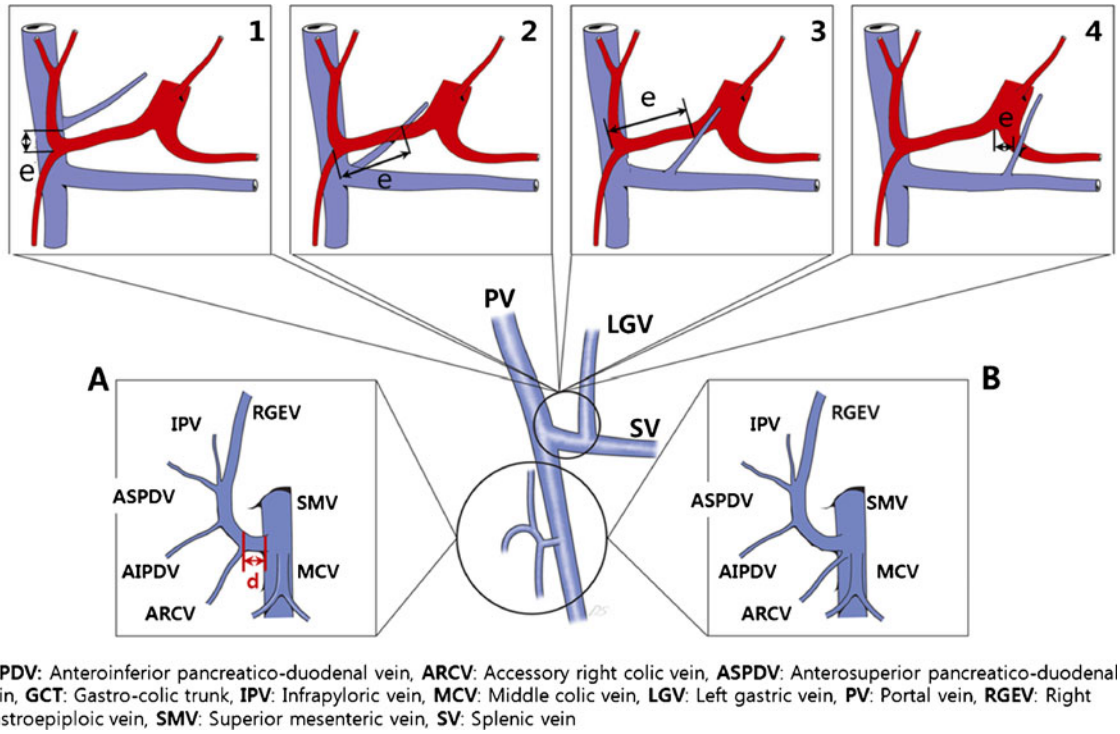


**Fig. 2** Estimation of venous components. Variations around the right gastroepiploic vein and left gastric vein were evaluated and distances from their reference points were measured (*d* length of gastrocolic trunk, *e* reference point for left gastric vein)

In four of the six vascular structures, the distance from each reference point to its origin was measured during surgery and compared with the findings from CT findings. We defined the four reference points as follows: (a) right gastroepiploic vein, where the gastrocolic trunk drains into the superior mesenteric vein; (b) right gastric artery, branch point of gastroduodenal artery and proper hepatic artery; (c) left gastric vein, branch point of gastroduodenal artery and proper hepatic artery in the case of portal vein drainage and the point at which the splenic artery and common hepatic artery begin to divide in the case of splenic vein drainage; (d) left gastric artery, the point at which the splenic artery and common hepatic artery begin to divide.

## Results

Characteristics of patients in this study are shown in Table 1. No patients had a co-morbid condition that would make robotic gastrectomy with lymph node dissection and preoperative CT with angiography unsafe. All examinations were performed and transferred to the surgeon's console successfully (Fig. 3, Videos 1–6).

Operative data and short-term outcomes are shown in Table 1. There was no open or laparoscopic conversion and no postoperative morbidity and mortality. All patients underwent curative R0 resection, and there was no combined resection or operation on other organs resulting from unintended vessel injuries. The mean number of harvested lymph nodes was 42±12.6. Mean operative time was 234.7±28.2 min and was approximately 15 min longer than that of our previous study (219.5±46.8 min).

Estimated blood loss was 46.4±12.6 mL. The median postoperative hospital stay was 6 days. No surgery-related morbidity, including liver dysfunction, pancreatitis, and anastomotic leakage occurred, and there was no surgery-related death.

In all patients, the stereoscopic vascular anatomy relating to the stomach was correctly identified and accurately rendered when compared with operative observations. All the vascular structures were precisely identified in all cases (Table 2).

The surgeon was able to identify the omental branch of the left gastroepiploic vessels (Video 1) and perform a partial omentectomy, preserving this branch in all 12 patients. There was no infarction of the remnant omentum. The mean length of the gastrocolic trunk was 14.5±3.9 mm (Video 2). In two cases, the accessory right colic vein and right gastroepiploic vein were not joined, and the gastrocolic trunk was absent. Instead, they drained into the superior mesenteric vein separately. In seven patients, the right gastroepiploic artery branched off the infrapyloric artery. In five patients, the gastroduodenal artery branched off the infrapyloric artery (Video 3). There was no erroneous damage to the accessory right colic vein or postoperative pancreatitis.

The right gastric artery originated from the proper hepatic artery in ten cases, bifurcated from the gastroduodenal artery in one case, and originated from the accessory left hepatic

**Table 1** Patients clinicopathologic characteristics (*N*=12)

| Characteristics | *N* (%) | Mean±SD | Range |
|---|---|---|---|
| Age (years) | | 61.1±10.9 | 43–75 |
| Gender (male–female) | 10:2 | | |
| BMI (kg/m$^2$) | | 23.6±1.8 | 19.2–26.2 |
| Co-morbidity | 5 (41) | | |
| Cardiovascular disease | 1 (8.3) | | |
| Pulmonary disease | 2 (16.7) | | |
| Renal disease | 1 (8.3) | | |
| Hepatic disease | 1 (8.3) | | |
| Previous abdominal surgery | 2 (11.8)[a] | | |
| Tumor location in stomach | | | |
| Middle | 3 (25) | | |
| Lower | 9 (75) | | |
| Number of retrieved lymph nodes | | 42.4±12.6 | 26–72 |
| Extent of lymph node dissection | | | |
| <D2 | 2 (16.7) | | |
| D2 | 10 (83.3) | | |
| Operation time (minutes) | | 234.7±28.2 | 194–296 |
| Estimated Blood Loss (mL) | | 46.4±12.6 | 23–84 |
| Resection margin (mm) | | | |
| Proximal | | 46.6±26.5 | 12–100 |
| Distal | | 50.9±26.5 | 28–120 |
| Stage | | | |
| Ia | 8 (66.7) | | |
| Ib | 3 (25) | | |
| III(c) | 1 (8.3) | | |
| Postoperative hospital stay (days) | | 6.0±2.0 | 5–11 |
| Postoperative complications | 0 (0.0) | | |

*N* number, *SD* standard deviation, *BMI* body mass index

[a]1 peritonitis, 1 appendectomy

artery from the left gastric artery in one case. The mean distance from the reference point to right gastric artery was 9.5±6.4 mm (Video 4).

The left gastric vein drained into the splenic vein in seven cases (Video 5), the portal vein in three, the confluence of the superior mesenteric vein and splenic veins in one, and the left portal vein in one. The mean distance from the branching point of the common hepatic artery and splenic artery to the left gastric vein was 15.9±10.3 mm, and in all seven cases, the left gastric vein crossed over anterior to the splenic artery and drained into the splenic vein. In the three cases of portal vein drainage, the average distance from the bifurcation of the gastroduodenal artery and proper hepatic artery was 26.8±2.4 mm, and the left gastric vein drained into the portal vein behind the proper hepatic artery or common hepatic artery.

The left gastric artery furnishing the aberrant left hepatic artery was successfully revealed; an accessory left hepatic artery in two cases and a replaced left hepatic in one case. The mean distance from the bifurcation of the common hepatic artery and splenic artery to the origin of the left gastric artery was 7.8±3.2 mm. The replaced left gastric artery was preserved during robotic gastrectomy, and information regarding these arteries enabled us to avoid accidental hemorrhage and ischemic liver damage during surgery (Video 6).

## Discussion

During this prospective observational study of gastric cancer patients undergoing elective CT image-guided robotic gastrectomy with lymph node dissection, we found that the vascular anatomy around the stomach was completely identified from preoperatively conducted CT images and all information were successfully transferred during operation. Surgeon received help from the images and did operations without fear of vascular injury, especially small or deep-seated vessels. Application of image-guided robotic gastrectomy for gastric cancer is clinically feasible and useful.

The significance of this study is the ability to present anatomical variations of an individual patient during the

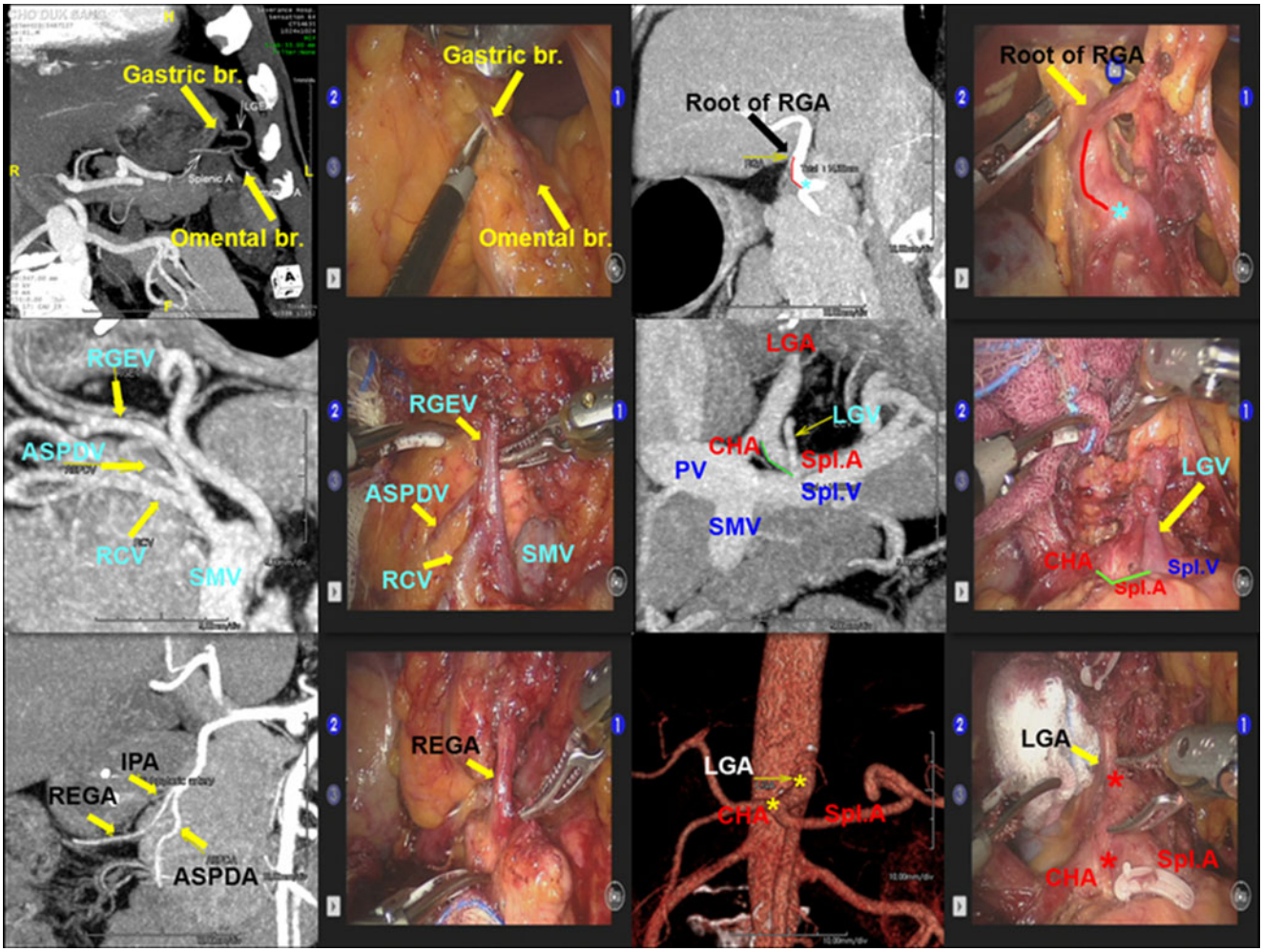


**Fig. 3** Intraoperatively provided preoperative CT images and matched operative findings of six vascular structures. *br* branch, *RGA* right gastric artery, *RGEV* right gastroepiploic vein, *ASPDV* anterosuperior pancreaticoduodenal vein, *RCV* accessory right colic vein, *SMV* superior mesenteric vein, *LGA* left gastric artery, *CHA* common hepatic artery, *LGV* left gastric vein, *PV* portal vein, *Spl.*A splenic artery, *Spl.V* splenic vein, *IPA* infrapyloric artery, *RGEA* right gastroepiploic artery, *ASPDA* anterosuperior pancreaticoduodenal artery, *LGA* left gastric artery

operation. Such variations are one of the major obstacles facing surgeons, especially in cancer surgery. In this study, 3D-reconstructed CT images integrated into the surgeon's robot console presented the variation of vessels around the stomach and abdominal aorta, which were different in all 12 patients of this study. Because these images show real, rather than statistical or textbook-based, anatomical variations, this information removes guesswork during the operation. Image-guided robotic surgery using preoperative CT scans therefore makes it easier and safer to perform more complicated minimally invasive surgery, especially for less experienced surgeons, because all surgeons have the same anatomical information regardless of surgical experience and knowledge of anatomy. Such information also makes it possible to perform patient-tailored surgeries based on one's individual anatomy.

Image-guided intervention techniques have been performed for about 20 years, and all utilize preoperatively acquired data, mostly in the form of tomographic images, combined with technology to link these images to the patient. Image guidance employs computer-based systems to help physicians precisely visualize and target the surgical site by providing virtual image overlays. Neurosurgeons use image guidance when they plan and simulate operations and perform functional surgery. The use of image-guided intervention techniques has expanded into orthopedics, cardiac, and thoracoabdominal areas.[7,9,16–21] Applications have been also extended beyond planning, simulating, and localization to treatment such as stent insertion and stereotactic surgeries.[12]

In clinical practice, image-guided surgery has been applied particularly successfully for bony structures such as the spine or for regions that are surrounded by a rigid enclosing structure such as the brain. However, for many surgical procedures, for example in the abdomen, the applications of image-guided surgery are limited to relatively

**Table 2** Observed data on 12 patients who underwent image-guided robot-assisted gastrectomy for gastric cancer in this study

| Patient no. | Sex | Age (years) | Omental branch of LGEA | RGEV drains into | Length of GCT | Infrapyloric artery from | RGA (mm) | Origin of RGA[b] | LGV drains into[c] | Distance to LGV (mm) | Distance to LGA (mm) | Left aberrant hepatic artery |
|---|---|---|---|---|---|---|---|---|---|---|---|---|
| 1 | Female | 66 | Identified | SMV | – | RGEA | 5.3 | Lateral | SV(a) | 6.2 | 10.4 | Absent |
| 2 | Male | 61 | Identified | GCT | 8.8 | RGEA | 15.6 | Medial | SV(a) | 13.3 | 10.7 | Absent |
| 3 | Male | 73 | Identified | GCT | 9.5 | RGEA | 14.8 | Medial | SV(a) | 14.0 | 7.5 | Absent |
| 4 | Male | 59 | Identified | GCT | 14.1 | RGEA | 8.0 | Medial | SV(a) | 4.5 | 0.0 | Absent |
| 5 | Male | 68 | Identified | SMV | – | GDA | 8.6 | Lateral | SV(a) | 12.7 | 7.9 | Absent |
| 6 | Male | 48 | Identified | GCT | 13.9 | GDA | 5.3 | Lateral | PV(p) | 27.3 | 5.2 | Absent |
| 7 | Male | 71 | Identified | GCT | 8.2 | GDA | 20.3[a] | Lateral | PV(p) | 33.9 | 6.2 | Accessory |
| 8 | Female | 58 | Identified | GCT | 12.5 | RGEA | 4.0 | Medial | Confluence[d] | 15.0 | 7.6 | Absent |
| 9 | Male | 75 | Identified | GCT | 5.7 | RGEA | 5.2 | Anterior | SV(a) | 23.2 | 5.8 | Replaced |
| 10 | Male | 66 | Identified | GCT | 18.3 | GDA | 14.8 | Medial | PV(p) | 19.2 | 10.7 | Accessory |
| 11 | Male | 43 | Identified | GCT | 8.5 | GDA | 22.8 | Medial | SV(a) | 37.1 | 12.6 | Absent |
| 12 | Male | 45 | Identified | GCT | 14.4 | RGEA | 0.0 | Anterior | LPV | – | 8.8 | Absent |
| Mean±SD | | | | | 9.5±5.4 | | 9.5±6.4 | | | | 7.8±3.2 | |
| Range | | | | | 5.7–18.3 | | 4.0–22.8 | | | | 5.2–12.6 | |

*LGEA* left gastroepiploic artery, *RGEV* right gastroepiploic vein, *GCT* gastrocolic trunk, *RGA* right gastric artery, *LGV* left gastric vein, *LGA* left gastric artery, *SMV* superior mesenteric vein, *RGEA* right gastroepiploic artery, *SV* splenic vein, *GDA* gastroduodenal artery, *PV* portal vein, *LPV* left portal vein, *SD* standard deviation

[a] Right gastric artery from the accessory left hepatic artery

[b] Side of the proper hepatic artery that the right gastric artery originates from

[c] The relative position of the left gastric vein to the common hepatic artery or splenic artery (a: anterior, p: posterior)

[d] The left gastric vein drains into the confluence of the superior mesenteric vein and splenic vein

fixed organs such as the kidney, liver, and spleen that show no positional changes during surgery. Current image guidance based on a formable and rigid-body model is not applicable to a hollow viscus.

The requirement for lymph node dissection around major vessels further restricts the applicability of image guidance to gastric cancer. For lymphadenectomy during gastric cancer surgery, it is necessary to know the location and direction of the vessels and the distance from the origin to resected sites. Accordingly, to apply image guided robotic gastrectomy for gastric cancer with preoperative CT images, we presumed that the location of vessels may change during gastrectomy, but the location of reference points and the length of vessels would not change. In this study, we investigated the feasibility of applying this navigation system using existing devices and software to the hollow viscus in abdominal surgery. Distances from the reference points were quantified, and 3D images from preoperative CT scan were converted to images that were registered with the real-time view of the surgeon during the operation. Although the peripheral regions of small vessels could not be visualized, very small vessels such as the right gastric artery (with a diameter less than 1 mm) could be identified and localized by measuring the distance from their reference points in the abdominal cavity. Synchronization of 3D CT images to the real-time view of the target anatomy through the same angle was adjusted for any discrepancies from the preoperative scan caused by positional changes. Measuring the distance from a reference point and maintaining the same angle alignment of 3D images makes it safe and easy to dissect the lymph nodes around the stomach. The mean operation time of the study (234.7±28.2 min) was approximately 15 min longer than that of our previous study (219.5± 46.8 min).[22] Although it takes an extra 15 min on average to perform robotic gastrectomy with this system, it would be acceptable increase of operation time considering additional benefits of this tool.

Image-based surgery using robotic surgery with TilePro™ is currently dependent on the skills of the radiologist. All the required images should be available at each operative step, and the radiologist must be able to manipulate the software and understand the surgical procedures in the operating room. Therefore, the first step in the establishment of image-based surgery will be automation of image reconstruction during surgery. Automation can be achieved by synchronization of camera position and the image reconstruction program. Simultaneously, simulation of the abdominal cavity after making a pneumoperitoneum has to be performed by calculating any position or distance changes resulting from the pneumoperitoneum. Such simulation could help guide the position of the trocar for every operation. This will be a basic system for intra-operative navigation. Analysis of the standardized image-based operation and simulation of the abdominal cavity can provide a simulation model. At this step, graphic rendering, 3D reconstruction of CT images for each organ, tissue specific properties, and operation procedure modeling should be incorporated to provide a good base for the application of image-guided surgery for various fields of abdominal surgery, such as colorectal, liver, and bilio-pancreas surgery.[23–25]

3D-to-3D image registration during the operation provides diverse information that is critical for surgical guidance and minimizes the risks involved in minimally invasive surgery. However, in this study, the images transferred were registered as 2D images at the surgeon's console after transferring through TilePro™, even though preoperative CT images were reconstructed in 3D. Because there were discrepancies between the 3D operative view and the presented 2D images at the robot console, a 3D display should be incorporated for future 3D-to-3D matching. We are currently developing 3D imaging software using preoperative CT scans that will make it possible to integrate 3D-to-3D at the robot console screen and assistant. In addition, improvement of virtual reality techniques and better quality CT scanning are required. Although our attempt is not a true image-guided surgery, it provides a transition to image-guided surgical planning and navigation for gastric cancer surgery.

## Conclusion

3D-reconstructed CT images provide vital information during surgery, in particular a vascular map that is critical for surgical guidance during lymphadenectomy and it minimizes the risk of vessel injury, especially of small or deep-seated vessels. This information can be combined with real-time information on deformable body structures. The application of image-guided robotic gastrectomy for gastric cancer using preoperative CT-angiography reconstructed during operation by a surgically trained radiologist who could adjust the images by anticipating the operative procedure is therefore both clinically feasible and valuable. Although further developments to the system are needed, image-guided robotic surgery could overcome many limitations of the minimally invasive surgical approach.

**Acknowledgments** The authors thank Dong-Su Jang Research Assistant, Department of Anatomy, Yonsei University College of Medicine, Seoul, Korea for his work on the illustrations of this article. The authors thank Katherine M Stefani English Editor, Yonsei University College of Medicine, Seoul, Korea for her work on the English proofreading of this article. This study was supported by a grant from the National R&D Program for Cancer Control, Ministry of Health and Welfare, Republic of Korea (1020410).

## References


1. Gybels J, Suetens P. Image-guided surgery. Verh K Acad Geneeskd Belg 1997;59(1):35–57; discussion 57–39
2. Vannier MW, Haller JW. Navigation in diagnosis and therapy. Eur J Radiol 1999;31(2):132–140.
3. Benabid AL, Hoffmann D, Le Bas JF, Lavallee S. Value of image guided neurosurgery in neuro-oncology. Bull Cancer 1995;82 Suppl 5:573 s-580 s.
4. Sugimoto M, Yasuda H, Koda K, et al. Image overlay navigation by markerless surface registration in gastrointestinal, hepatobiliary and pancreatic surgery. J Hepatobiliary Pancreat Sci 2010;17 (5):629–636.
5. Rassweiler J, Baumhauer M, Weickert U, et al. The role of imaging and navigation for natural orifice translumenal endoscopic surgery. J Endourol 2009;23(5):793–802.
6. Lim JS, Hyung WJ, Park MS, Kim MJ, Noh SH, Kim KW. Imaging-guided minimally invasive laparoscopic resection of intraluminal small-bowel tumor: report of two cases. AJR Am J Roentgenol 2007;189(1):56–60.
7. Marescaux J, Solerc L. Image-guided robotic surgery. Seminars in laparoscopic surgery 2004;11(2):113–122.
8. Maciunas RJ. Computer-assisted neurosurgery. Clin Neurosurg 2006;53:267–271.
9. Yeniaras E, Deng Z, Syed MA, Davies MG, Tsekos NV. A novel virtual reality environment for preoperative planning and simulation of image guided intracardiac surgeries with robotic manipulators. Stud Health Technol Inform 2011;163:716–722.
10. Shamir R, Freiman M, Joskowicz L, Shoham M, Zehavi E, Shoshan Y. Robot-assisted image-guided targeting for minimally invasive neurosurgery: planning, registration, and in-vitro experiment. Med Image Comput Comput Assist Interv 2005;8(Pt 2):131–138.
11. Chandra V, Dutta S, Albanese CT. Surgical robotics and image guided therapy in pediatric surgery: emerging and converging minimal access technologies. Semin Pediatr Surg 2006;15 (4):267–275.
12. Kumano S, Tsuda T, Tanaka H, et al. Preoperative evaluation of perigastric vascular anatomy by 3-dimensional computed tomographic angiography using 16-channel multidetector-row computed tomography for laparoscopic gastrectomy in patients with early gastric cancer. J Comput Assist Tomogr 2007;31(1):93–97.
13. Matsuki M, Tanikake M, Kani H, et al. Dual-phase 3D CT angiography during a single breath-hold using 16-MDCT: assessment of vascular anatomy before laparoscopic gastrectomy. AJR Am J Roentgenol 2006;186(4):1079–1085.
14. Hawkes DJ, Barratt D, Blackall JM, et al. Tissue deformation and shape models in image-guided interventions: a discussion paper. Med Image Anal 2005;9(2):163–175.
15. Song J, Oh SJ, Kang WH, Hyung WJ, Choi SH, Noh SH. Robot-assisted gastrectomy with lymph node dissection for gastric cancer: lessons learned from an initial 100 consecutive procedures. Ann Surg 2009;249(6):927–932.
16. Ahrar K, Wallace M, Javadi S, Gupta S. Mediastinal, hilar, and pleural image-guided biopsy: current practice and techniques. Semin Respir Crit Care Med 2008;29(4):350–360.
17. Hong K, Georgiades CS, Geschwind JF. Technology insight: Image-guided therapies for hepatocellular carcinoma–intra-arterial and ablative techniques. Nat Clin Pract Oncol 2006;3(6):315–324.
18. Matsuki M, Kanazawa S, Kanamoto T, et al. Virtual CT gastrectomy by three-dimensional imaging using multidetector-row CT for laparoscopic gastrectomy. Abdom Imaging 2006;31(3):268–276.
19. Pandya S, Motkoski JW, Serrano-Almeida C, Greer AD, Latour I, Sutherland GR. Advancing neurosurgery with image-guided robotics. J Neurosurg 2009;111(6):1141–1149.
20. Paul HA, Bargar WL, Mittlestadt B, et al. Development of a surgical robot for cementless total hip arthroplasty. Clin Orthop Relat Res 1992(285):57–66.
21. Tseng CS, Chung CW, Chen HH, Wang SS, Tseng HM. Development of a robotic navigation system for neurosurgery. Stud Health Technol Inform 1999;62:358–359.
22. Woo Y, Hyung WJ, Pak KH, et al. Robotic gastrectomy as an oncologically sound alternative to laparoscopic resections for the treatment of early-stage gastric cancers. Arch Surg 2011;146 (9):1086–1092.
23. Cleary K, Peters TM. Image-guided interventions: technology review and clinical applications. Annu Rev Biomed Eng 2010;12:119–142.
24. Kwartowitz DM, Miga MI, Herrell SD, Galloway RL. Towards image guided robotic surgery: multi-arm tracking through hybrid localization. Int J Comput Assist Radiol Surg 2009;4(3):281–286.
25. Mirota DJ, Ishii M, Hager GD. Vision-based navigation in image-guided interventions. Annu Rev Biomed Eng 2011;13:297–319.